

Supplementary material

Experimental and Density Functional Study of the Light Assisted Gas-Sensing Performance of a TiO₂–CoFe₂O₄ Heterojunction

Wenhao Wang,^a Lu Zhang,^{*b} Yanli Kang,^a Xiaodong Yang,^{*c} Shenguang Ge,^d and Feng Yu^{*a}

^a Key Laboratory for Green Processing of Chemical Engineering of Xinjiang Bingtuan, School of Chemistry and Chemical Engineering, Shihezi University, Shihezi 832003, P.R. China. E-mail: yufeng05@mail.ipc.ac.cn

^b Institute of Materia Medica, Xinjiang University, Urumqi 830017, China. E-mail: zhanglu@xju.edu.cn

^c Key Laboratory of Ecophysics and Department of Physics, College of Science, Shihezi University, Xinjiang 832003, P.R. China. E-mail: yangxiaodong1209@hotmail.com

^d Institute for Advanced Interdisciplinary Research, University of Jinan, Jinan 250022, P.R. China.

Experimental section

Preparation of CoFe₂O₄ and TiO₂–CoFe₂O₄

The cobalt chloride and ferric chloride were mixed in a ratio of 1:2 (molar ratio) and added to a solution of ethylene glycol and sodium acetate. The resulting solution was stirred and then allowed to stand for one night. Thereafter, the suspension was hydrothermally treated at 180 °C for 24 h. Then, the solution was cooled to room temperature, centrifuged and washed with a large amount of deionized water and anhydrous ethanol. Finally, the obtained product was dried at 60 °C to obtain CoFe₂O₄.

The preparation method of TiO₂–CoFe₂O₄ heterostructure was similar to that of CoFe₂O₄ except that the same molar amount titanium dioxide suspension was added before the hydrothermal treatment.

Materials characterization

X-ray diffraction (XRD) analysis was performed using an X-ray diffractometer (BRUCKERD8 ADVANCE) with Cu K α radiation (TiO₂) and Co K α radiation (CoFe₂O₄, TiO₂–CoFe₂O₄ heterojunction) at a scan rate of 8°/min. The chemical nature of all samples was studied using X-ray photoelectron spectrophotometry (XPS) with Thermo escalab 250Xiequipment. The morphologies and structures of the as-prepared samples were analyzed using field-emission scanning electron microscopy (FESEM, SU8020). Transmission electron microscopy (TEM) and high-resolution TEM (HRTEM) images were observed using an FEI Tecnai G2 F30 transmission electron microscope. Specific area and pore diameter distributions were estimated using the Brunauer–Emmett–Teller (BET) equation and Barrett–Joyner–Halenda (BJH) method based on the N₂ adsorption–desorption isotherm (ASAP 2460). UV–visible diffuse reflectance spectra (UV–vis DRS) of the samples were recorded using an ASAP 2460 instrument. An FLS1000/FS5 fluorescence spectrometer (wavelength = 350 nm) was used to obtain the photoluminescence (PL) spectra, which was used to analyze the recombination behavior of photoinduced carriers.

Sensing performance evaluation

The sensing performance in this work was evaluated by a CGS-8 intelligent gas-sensing system (Beijing Elite Co., Ltd.). Before the test, the gas-sensitive material was mixed with ethanol and dropped onto the surface of a ceramic tube that was welded to a hexapod base. After the surface of the ceramic tube dried, it was aged at 150 °C for 48 hours. In addition, the gas-sensing performance under light excitation was performed by using a LEDs-based lamp that was placed above the sensor with distance of ~3 cm. The measured light intensity of each wavelength irradiated on the surface of the sensor material was ~3.6 mW/cm². The response of the sensors was calculated using the following equation:

$$\text{Response} = R_a/R_g \quad (1)$$

where R_a and R_g are the sensor resistances in air and in the tested gas, respectively.

Furthermore, during the gas-sensitivity test, a quantitative liquid was added to the liquid evaporator (the test system was equipped with corresponding calculation software, and when the volume of the gas chamber, the concentration of the gas to be

measured, and various physical and chemical properties of the dripping liquid were input, the volume of the liquid to be dripped was obtained). The liquid was evaporated using an internal fan system to make it uniformly diffuse in the gas chamber and form a certain concentration of tested gas. The temperature of the evaporation platform was fixed at ~ 250 °C. All sample gases were obtained in this way. The total volume of the measurement chamber is 1 L. When the test gas is removed, it is only necessary to open the air chamber and turn on the fan in the chamber, and thus the test gas is discharged and the outside ambience enters. Among gases, NH_3 was prepared by evaporating ammonia with a concentration of 25%, which was then dropped on the evaporation platform in the gas chamber.

Theoretical calculation parameters

The Vienna Ab initio Simulation Package (VASP)[1] was used to perform the ab initio density functional theory (DFT)[2] calculations. The projector augmented wave[3] method was used to describe the interactions between valence and core electrons. The electronic exchange–correlation energy was calculated using the generalized gradient approximation (GGA)[4] of the Perdew–Burke–Ernzerhof (PBE)[5] functional. The PBE functional with the vdW correction (DFT–D2)[6] was used to describe the interfacial interactions of the vdW heterostructures. All slabs with a net dipole moment were calculated with the dipole correction. Gamma-centered k-point meshes in the first Brillouin zone were set to $10 \times 10 \times 1$ for all structures. The vacuum layer was set to 20 Å along the z-direction to avoid spurious interactions between the neighboring slabs. For the geometry optimization, the convergence criteria of energy and force were set to 10^{-8} eV and 10^{-6} eV Å $^{-1}$, respectively.

Results and discussion

Structural and morphological characterization

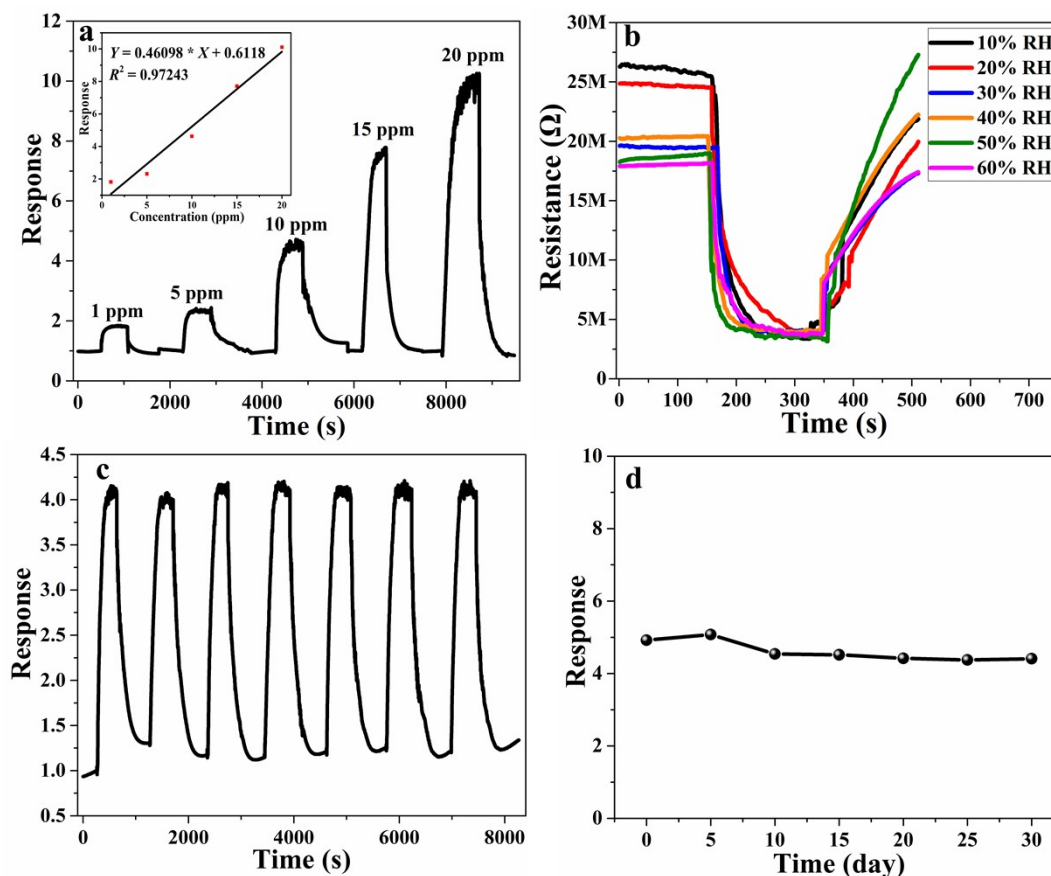


Fig. S1. a Dynamic response of $\text{TiO}_2\text{-CoFe}_2\text{O}_4$ heterostructure to toluene (inset: fitted curves of the sensor responses with toluene concentrations), b influence of relative humidity (RH) on the resistance of $\text{TiO}_2\text{-CoFe}_2\text{O}_4$ heterostructure to toluene gas, and c reproducibility and d long-term stability of $\text{TiO}_2\text{-CoFe}_2\text{O}_4$ heterostructure to toluene at 219 °C.

Fig. S1.a presents the dynamic response curves of TiO₂-CoFe₂O₄ heterostructure. The response value increased from 1.8 to 10 with increasing acetone concentration (1 to 20 ppm). In addition, the limit of detection (LOD) can be estimated as 3δ/s based on linear fitting, in which

$$\delta = \sqrt{\frac{\sum_{i=1}^n (x_i - \bar{x})^2}{n-1}}$$

δ is the standard deviation () and s is the slope of the linear fit [62]. The LOD of TiO₂-CoFe₂O₄ heterostructure to toluene was calculated as ~27 ppb.

Furthermore, the influence of relative humidity (RH) on the resistance of the TiO₂-CoFe₂O₄ heterostructure was tested (Fig. S1.b). In this work, the experiment was conducted in the northwestern region of China where the air is relatively dry and the RH value is ~10% (RH can be directly read on the control panel of the equipment). During the test, it was only necessary to evaporate a certain amount of distilled water into the gas chamber until the control panel displayed the required RH. The response value of the TiO₂-CoFe₂O₄ heterostructure to 15-ppm toluene decreased from ~9.7 to ~4.5 with rise in RH. The possible reason for this phenomenon was that water vapor molecules occupied the adsorption sites on the gas-sensitive material. This affected the adsorption and reaction of oxygen and toluene, resulting in a decrease in the response value. Furthermore, the adsorbed water molecules would interact with active oxygen species, releasing electrons to the conduction band of the gas-sensitive material[63]. Therefore, the Ra value would also be reduced as RH increased.

Afterward, the repeatability and long-term stability of the material were tested (Fig. S1.c and d). It can be seen that the response value of TiO₂-CoFe₂O₄ heterojunction was stable at ~4 to 10-ppm toluene for seven cycles and the baseline does not drift considerably. In addition, the long-term stability of TiO₂-CoFe₂O₄ heterojunction to 10-ppm toluene gas was tested every 5 days. The results revealed that the response value was maintained at ~80% (compared with the initial response) after 30 days.

References

- [1] P. E. Blochl, Projector augmented-wave method, *Phys. Rev. B: Condens. Matter* 50 (1994) 17953-17979.
- [2] P. Hohenberg, W. Kohn, Density Functional Theory (DFT), *Phys. Rev.* 136 (1964) B864-B892.
- [3] G. Kresse, D. Joubert, From ultrasoft pseudopotentials to the projector augmented-wave method, *Phys. Rev. B* 59 (1999) 1758-1776.
- [4] W. Kohn, L. J. Sham, Self-Consistent Equations Including Exchange and Correlation Effects, *Phys. Rev.* 140 (1965) A1133-A1138.
- [5] M. C. Payne, M. P. Teter, D. C. Allan, T. A. Arias, J. D. Joannopoulos, Iterative minimization techniques for ab initio total-energy calculations: molecular dynamics and conjugate gradients, *Rev. Mod. Phys.* 64 (1992) 1045-1097.
- [6] S. Grimme, Semiempirical GGA-type density functional constructed with a long-range dispersion correction, *J. Comput. Chem.* 27 (2006) 1787-1799.